Peripheral and central alterations affecting spinal nociceptive processing and pain at adulthood in rats exposed to neonatal maternal deprivation

(Article begins on next page)

07 January 2023

Peripheral and central alterations affecting spinal nociceptive processing and pain at adulthood in rats exposed to neonatal maternal deprivation

Pierre-Eric Juif,[1] Chiara Salio,[2] Vivien Zell,[1] Meggane Melchior, [1] Adrien Lacaud,[1] Nathalie Petit-Demouliere,[1] Francesco Ferrini,[2] Pascal Darbon,[1] Ulrike Hanesch,[3] Fernand Anton,[3] Adalberto Merighi,[2] Vincent Lelievre[1] and Pierrick Poisbeau[1]

[1]Institute of Cellular and Integrative Neurosciences (INCI), Centre National de la Recherche Scientifique, University of Strasbourg, 5 Rue Blaise Pascal, F-67084 Strasbourg, France

[2]Department of Veterinary Sciences, Universita degli Studi di Torino, Torino, Italy

[3]Laboratory of Neurophysiology and Psychobiology, University of Luxembourg, Luxembourg, Luxembourg

Corresponding author

Prof. Pierrick Poisbeau, Institut des Neurosciences Cellulaires et Intégratives (INCI), CNRS UPR 3212, 5 rue Blaise Pascal, 67084 Strasbourg, France ; Tel:(+33)368851476 - Fax:(+33)388613347; E-mail: poisbeau@inci-cnrs.unistra.fr.

Abstract

The nociceptive system of rodents is not fully developed and functional at birth. Specifically, C fibers transmitting peripheral nociceptive information establish synaptic connections in the spinal cord already during the embryonic period that only become fully functional after birth. Here, we studied the consequences of neonatal maternal deprivation (NMD, 3 h/day, P2–P12) on the functional establishment of C fiber-mediated neurotransmission in spinal cord and of pain-related behavior. In vivo recording revealed that C fiber-mediated excitation of spinal cord neurons could be observed at P14 only in control but not in NMD rats. NMD was associated with a strong alteration in the expression of growth factors controlling C nociceptor maturation as well as two-pore domain K+ channels known to set nociceptive thresholds. In good agreement, C-type sensory neurons from NMD animals appeared to be hypoexcitable but functionally connected to spinal neurons, especially those expressing TRPV1 receptors. In vivo and in vitro recordings of lamina II spinal neurons at P14 revealed that the NMD-related lack of C fiber-evoked responses resulted from an inhibitory barrage in the spinal cord dorsal horn. Eventually, C-type sensory-spinal processing could be recovered after a delay of about 10 days in NMD animals. However, animals remained hypersensitive to noxious stimulus up to P100 and this might be due to an excessive expression of Nav1.8 transcripts in DRG neurons.

Together, our data provide evidence for a deleterious impact of perinatal stress exposure on the maturation of the sensory-spinal nociceptive system that may contribute to the nociceptive hypersensitivity in early adulthood.

Introduction

The development of the spinal nociceptive system and of pain responses follows a parallel trajectory in humans and rats. Whereas C fibers become fully mature during the last trimester of gestation in humans (White & Wolf, 2004), it is generally assumed that the nociceptive system matures during the first three postnatal weeks in the rat (Bayer et al., 1993). A functional glutamatergic sensory-spinal transmission mediated by C-type primary afferent fibers (PAFs) has been demonstrated a few days after birth (Baccei et al., 2003). At the same period, inhibitory controls mediated by $GABA_A$ and glycine receptors are submitted to major plastic changes which affect synapse selectivity (Keller et al., 2001; Baccei & Fitzgerald, 2004) and chloride homeostasis (Rivera et al., 1999; Li et al., 2002; Stil et al., 2009). However, functional glutamatergic excitation resulting from C-type stimulation is apparently not sufficient to trigger action potentials (APs) in superficial dorsal horn cells before P10 (Fitzgerald, 1988; Jennings & Fitzgerald, 1998).

Nerve growth factor (NGF) and glial-derived neurotrophic factor (GDNF) play crucial roles in the complex reorganization of the spinal sensory pathways occurring after birth. NGF and GDNF control the anatomical pattern and density of sensory innervation as well as the physiological phenotype of sensory neurons, and, specifically related to the context of this work, the survival/maturation of nociceptive C fibers (Ruit et al., 1992; Bennett et al., 1996; Fitzgerald, 2005). All newly formed embryonic C-type nociceptors express the NGF receptor trkA, but, during the early postnatal period, about half of them switch off the trkA gene and starts expressing the GDNF receptor RET (Fitzgerald, 2005). These neurons eventually become non-peptidergic C-nociceptors, and can be labeled by the isolectin B4 (IB4), whereas the C-nociceptors retaining trkA start expressing the calcitonin gene-related peptide (CGRP) and thus become C-nociceptors of the peptidergic type (Fitzgerald, 2005).

Neonatal maternal deprivation (NMD) is an established model for assessing the effect of adverse early life experiences that induce neuroendocrine and behavioral changes in rats persisting throughout life. Studies using a separation paradigm of 3 h/day, from P2 to P12, have shown that NMD induces alterations that can still be observed in adults. Indeed, it has been well established that NMD affects social behaviors (Kikusui & Mori, 2009), is associated with hyperreactivity of the hypothalamo–pituitary–adrenal axis (Plotsky & Meaney, 1993; Ladd et al., 2000) and visceral hyperalgesia to colon distension (Chung et al., 2007; Schwaller & Fitzgerald, 2014). NMD-induced visceral hyperalgesia in adulthood has also been shown to be associated with alterations of NGF expression (Chung et al., 2007; Tsang et al., 2012).

In this work, we used in vivo and in vitro electrophysiological recordings from spinal cord dorsal horn and dorsal root ganglion (DRG) neurons to characterize the early consequences of NMD on sensory-spinal transmission and integration. Behavioral measures of mechanical and thermal nociceptive thresholds helped to characterize long-term consequences of NMD. This approach was complemented by the analysis of C fiber neurochemical markers and growth factor expression in the spinal cord to identify the biochemical pathways potentially underlying the plastic mechanisms induced by NMD.

Material and methods

Animals

Female Sprague–Dawley rats (Janvier, Le genest St Isle, France) with litters were housed in a temperature-controlled room (22 °C) under a 12-h light–dark cycle (lights on at 07:00 h), with ad libitum access to food and water. All experiments were conducted in conformity with the directive (2010/63/EU) of the European Parliament and of the Council of September 22, 2010, with an authorization for animal experimentation from the French Department of Agriculture (License 67-116 to PP) and with a procedure agreement granted by the regional ethical committee (authorization number AL/01/01/02/11).

Neonatal maternal deprivation

At birth, litters were randomly assigned to two groups, NMD and controls, following a previously published procedure (Plotsky & Meaney, 1993). Litters allocated to the NMD group were removed from the nest cages 3 h/day from P2 to P12 and placed on a heating pad (37 °C) in a separate cage. Litters allocated to the control group remained with the mother in their home cages during the entire NMD interval and received no special handling other than that necessary to change the bedding twice a week. Because initial experiments for which male or female rats were randomly chosen failed to detect any significant sex-specific differences, data were pooled together.

Preparation of the spinal cord and in vivo recordings

The preparation of the spinal cord and the in vivo recordings was done as previously described (Juif & Poisbeau, 2013). Rats were initially anaesthetized with isoflurane (3%; pushed by pure oxygen at a flow rate of 0.5 L/min). This concentration was then reduced to 2% isoflurane for the ensuing surgery. The body temperature was regulated using a thermostatically controlled heating blanket (Harvard Apparatus Ltd) maintaining the core temperature of 37 °C. Animals were set up in an animal stereotaxic frame (La Precision Cinematographique, France), with the cervical and sacral vertebrae firmly held. The lumbar spinal cord was exposed by laminectomy, the dura mater and arachnoids were removed, and the cord was covered with a thin isolating lamina of mineral oil. This opening allowed us to apply drugs directly to the spinal cord. At the end of the experiment, animals were killed with an overdose of isoflurane.

Electrophysiological recordings and analysis

Single-unit extracellular recordings were made from convergent dorsal horn neurons, also called "wide dynamic range" (WDR) neurons, located in the deep laminas of the lumbar spinal cord (L4–L5) using stainless steel microelectrodes (FHC, Bowdoin, ME, USA) connected to an extracellular differential amplifier (DAM-80, WPI, Aston, UK). Electrical signals were then digitized (Power 1401 CED, Cambridge, UK), visualized, and stored on a

personal computer equipped with the SPIKE 2 software (CED). Neurons were identified by means of natural (brush or pinch) stimuli and then characterized by their responses to transcutaneous electrical stimulation of the hindpaw receptive field.

Electrical stimulation was applied through two thin pin electrodes inserted into the skin and placed in the center of the receptive field (RF). Isolated stimulation with increasing intensities was applied with voltage ranging from 1 to 99 V (duration of 1 ms) to trigger the appearance of a C-type fiber-related action potential discharge and to measure its threshold. Trials consisting of a train of 30 suprathreshold electrical stimuli applied repetitively (1 Hz) to the receptive field were used to obtain a stable and reproducible "wind up", as previously described (Mendell, 1966). The electrically evoked response of the neuron was captured and displayed as a post-stimulus histogram (PSTH). This allowed the quantification of response latency and of A and C fiber thresholds. Adjustments were commonly made for neonatal animals based on the size of the animal (Urch & Dickenson, 2003): A fiber-evoked responses were measured from 0 to 50 ms, C fiber- and post-discharge–evoked responses from 50 to 800 ms. To evaluate the windup efficiency, the mean response observed for the 30 stimulations was calculated and related to the "input" value (i.e., response to an isolated stimulation 9 number of stimulations).

A similar method was applied to record from DRG neurons. Unit recording of C-type neurons was confirmed based on their conduction velocity and the corresponding latency to observe an action potential discharge after stimulation of the paw receptive field. The receptive field was also chemically stimulated by applying a 50 µL drop of capsaicin (0.5%) directly on the paw skin.

Patch-clamp recordings and analysis

Slice preparation and solutions

Transverse slices were prepared as described previously in detail (Keller et al., 2001). The spinal cord was removed and immediately immersed in cold (4 °C) sucrose-based artificial cerebrospinal fluid (ACSF) containing (in mM): 248 sucrose, 11 glucose, 26 $NaHCO_3$, 2 KCl, 1.25 KH_2PO_4, 2 $CaCl_2$, and 1.3 $MgSO_4$ continuously bubbled with 95% O_2–5% CO_2, pH 7.35. The lumbar segment was glued vertically on an agarose block (5.5%) with cyanoacrylate prior to mounting on the platform of a tissue slicer chamber (Leica 1100vs, Germany). Transversal slices (600 lm thick) were cut from the lumbar segment with a tissue slicer (Leica VT1000S, Wetzlar, Germany) and stored at room temperature in ACSF containing 126 mM of NaCl instead of sucrose. After at least 1 h, slices were transferred to the recording chamber and continuously perfused with oxygenated ACSF.

Electrophysiological recordings and data acquisition

Whole-cell voltage clamp recordings were obtained with an Axon MultiClamp 700B amplifier (Axon Instruments, Foster City, CA, USA). Borosilicate glass electrodes (R = 3–8 MO) with inner filament (1.2 outer diameter to 0.69 inner diameter; Harvard Apparatus Ltd, UK) were pulled using a horizontal laser puller (P2000; Sutter Instruments, CO, USA). Pipettes were filled with an intracellular solution containing (in mM): 80 Cs_2SO_4, 2 $MgCl_2$, 8 KCl, 10

HEPES, 2 MgATP, 0.2 NaGTP. The pH 7.3 was adjusted using a CsOH solution (1 mM). Under these conditions (i.e. low intracellular concentration of chloride ions; ECl = 60 mV) and at a holding potential of 0 mV, we selectively isolated inhibitory postsynaptic currents (IPSCs) that were seen as outward currents. IPSCs corresponded to the synaptic activation of glycine and GABAA receptor channels, sensitive to strychnine (1 lM) and bicuculline (10 lM), respectively. Excitatory postsynaptic channels (EPSCs) were recorded at a holding potential of 60 mV. All recordings were performed at room temperature. Series capacitances and resistances were compensated electronically throughout the experiments using the main amplifier. Recordings were filtered at 2 kHz, digitized at 10 kHz and stored on computer using PCLAMP 8.0 software (Molecular Devices, Sunnyvale, CA, USA) before being analyzed.

Data analysis

Spontaneous synaptic currents were detected and analyzed using the Strathclyde electrophysiology software packages WINEDR and WINWCP (courtesy of Dr J. Dempster, University of Strathclyde, Glasgow, UK). Detection of each single event was further confirmed by visual inspection. For each synaptic current, the peak amplitude, the current charge (area) and the monoexponential deactivation constant (s decay) were measured.

Immunofluorescence (IMF)

Tissue fixation

P14 rats (n = 10) were deeply anesthetized with an intraperitoneal injection of pentobarbital (100 mg/kg; Ceva Sante Animale, France). Animals were perfused transcardially with an initial solution of tyrode (pH 7.3) and heparin (Heparin-Natrium, Braun 10 000 I.E./mL, 2 mL/L) followed by fixative consisting of 4% paraformaldehyde in 0.1 M phosphate buffer saline (PBS; pH 7.4). Lumbar spinal cord segments and dorsal root ganglia (DRGs) were removed and post-fixed overnight in the same fixative and stored at 4 °C in PBS.

Tissue preparation

Lumbar spinal cord segments and DRGs were dehydrated and embedded in paraffin wax. Transverse sections were cut at 6 μm with a microtome (Leica Microsystems, RM 2125RT).

IMF

Sections from CT and NMD animals were processed together. Sections were deparaffinized, rehydrated, washed in PBS and pre-incubated for 1 h in PBS containing 6% bovine serum albumin, processed for microwave antigen retrieval for 10 min in 10 mM sodium citrate buffer pH 6.0, and then incubated overnight at room temperature in a mixture of rabbit anti-CGRP antibody (1 : 1000, Sigma, St. Louis, MO, USA, catalog number: C8198) and biotiny-lated lectin Griffonia simplicifolia (IB4) (1 : 250; Sigma, catalog number: L2140). Sections were then rinsed in PBS

and incubated for 1 h in a mixture of an anti-rabbit secondary antibody IgG Alexa Fluor 594 (1 : 500; Invitrogen, Molecular Probes, Eugene, OR, USA) and Extravidin FITC (1 : 500; Sigma). Sections were washed in PBS and mounted in Fluoroshield (Sigma). Routine immunocytochemical controls consisted in omission of primary antibodies (Salio et al., 2005).

To identify the Rexed lamination in the spinal cord, a triple fluorescence labeling was also performed following a protocol previously described (Lorenzo et al., 2008). Briefly, after sections were brought to PBS they were incubated in Red Neurotrace Fluorescent Nissl (1 : 200; Invitrogen, Molecular Probes) for 20 min at room temperature; and then immunostained as described above using a blue anti-rabbit secondary antibody IgG Alexa Fluor 633 (1 : 500, Invitrogen, Molecular Probes) instead of the red IgG Alexa Fluor 594. All immunostaining protocols were repeated twice for each animal by using different sections. Results obtained in each experimental session were averaged.

Microscopy image analysis and quantification

Sections of both spinal cord (n = 4 control and n = 5 NMD rats) and DRGs (n = 5 control and n = 5 NMD rats) were observed with a confocal laser scanning microscope (Leica Microsystems, TCS SP5). Sections were photographed as single-stack images at 209 (pixel size 757 nm) and pairs of digital images of the same microscopic field were obtained with appropriate filter combinations to visualize the fluorescence labels. Laser parameters were kept unchanged for the different experimental conditions (CT vs. NMD) so that the detection of staining was maximal while avoiding pixel saturation.

Quantitative analysis was performed by an operator unaware of the experimental group. Images were analyzed with IMAGEJ software (NIH, Bethesda, MD, USA). For spinal cord quantification, a total of 40 randomly chosen sections from four control rats (~ 10 sections/rat) and 78 sections for five NMD rats (~ 15 sections/rat) were analyzed. For DRGs quantification, 2–3 lumbar DRGs per rat were serially sectioned in toto at 6 lm, and one of five sections in the series was used for immunostaining. A total of 264 sections from five control rats (~ 53 sections/rat) and 226 sections from five NMD rats (~ 45 sections/rat) were analyzed.

Mean fluorescence intensity, fluorescent DRG cells and dorsal horn (lamina I and II) areas were measured. In the dorsal horn, mean fluorescence intensity was estimated by subtracting the background mean value from the overall mean grey value; in DRGs, by setting a threshold twice the value of background mean grey value to objectively discriminate positive cell bodies from negative ones (Bertin et al., 2013). Integrated density was calculated as mean fluorescence intensity 9 area, thus confining the selection to the cell soma. The number of positive cells in DRGs was automatically determined by setting the ImageJ particle analyzer to detect nearly circular objects of about 100–700 lm^2 area and by limiting the analysis to the thresholded area (see above). Cell densities were expressed as number of positive cells/mm^2. Data were pooled by rat and averaged values were used for subsequent statistical analysis.

PCR

Lumbar spinal cord was collected, flash frozen with dry ice and stored at – 80 °C. Total RNA was extracted according to a protocol consisting of two independent total RNA extractions separated by a DNAseI treatment (DNA free kit,

Ambion; Life Technologies, Saint Aubin, France) as previously described in detail (Lelievre et al., 2002). RNA quality and concentration were assessed by spectrophotometry and automated electrophoresis on microfluidic chips (Agilent 2100 Bioanalyzer system; Agilent Technologies, Les Ulis, France). Total RNA (800 ng/sample) was subjected to reverse transcription using the Iscript kit according to the manufacturer instructions (Bio-Rad, Marnes-la-coquette, France). PCR was set up in 96-well plates using diluted cDNA samples, highly selective primer sets and SyberGreen-containing PCR reagents (Bio-Rad) accurately dispensed using a robotic workstation (Freedom EVO100 from Tecan, Lyon, France). Gene amplification and expression was performed on a MyIQ real-time PCR machine (Bio-Rad) using a three-step procedure (15 s at 96 °C; 10 s at 62 °C; 15 s at 72 °C) followed by a melting curve study to ensure specificity of the amplification process. Standardization was made possible using standard curves made from control RNA samples. Preliminary experiments showed that 18S, GAPDH (glyceraldehyde 3-phosphate dehydrogenase) and HPRT (hypoxanthine-guanine phosphoribosyltransferase) levels remained highly stable among the different samples and treatment conditions. The latter housekeeping gene was therefore chosen to standardize all the quantitative experiments presented here. The differences between samples were calculated on the basis of the specific ratios (gene of interest/housekeeping gene).

Behavioral testing

Habituated adult Sprague–Dawley rats (n = 6/group) were used to measure nociceptive thresholds while applying mechanical and thermal heat stimuli on their hind paws. All behavioral tests were done between 9:00 and 16:00 h, i.e. during the light period. Mechanical sensitivity was measured using a calibrated forceps (Bioseb, Vitrolles, France) previously validated in our laboratory (Luis-Delgado et al., 2006). Briefly, the rat was loosely restrained with a towel masking the eyes to limit stress by environmental stimulations. The tips of the forceps were placed on each side of the hind paw and a gradually increasing force was applied. The pressure level inducing paw withdrawal indicated the nociceptive threshold value. The thermal heat nociceptive response was assessed using Hargreaves' test (Bioseb, Vitrolles, France), allowing to differentiate the response to stimulation of each hind paw (Hargreaves et al., 1988). Hind paws were exposed to a radiant heat and the time latency required to induce paw withdrawal from the surface was taken as the noxious heat threshold. Noxious pressure threshold or withdrawal latency measurements were performed three times for each hind paw and the values were averaged.

Statistical analysis

All data are expressed as mean SE of the mean (SEM). According to need, we used parametric (Two-tailed Student's t-test) or non-parametric (Mann–Whitney) statistical tests. A two-way ANOVA followed by Tukey multiple comparison post hoc test helped to reveal differences between C fiber threshold values, whereas a similar test, with repeated measures, followed by Bonferroni multiple comparison test was used to analyze (i) the transcript changes for growth factors and receptors during development and (ii) nociceptive thresholds with postnatal age. Differences were considered to be statistically significant for $P < 0.05$.

Results

Establishment of functional C-type sensory-spinal transmission

In control animals and in good agreement with the existing literature, C fiber-mediated transmission appeared to be fully functional in the spinal cord of P14 control rats (Fig. 1A). After stimulation of the peripheral RF, we observed a C-type action potential discharge while recording from single neurons from superficial (n = 7/7; depth: 98 ± 13 µm, not shown) and deep (n = 18/20; depth: 450 ± 89 µm; Figure 1A) dorsal horn laminas. In NMD animals at P14, we failed to see any C fiber discharge in superficial laminas (0/13; mean depth: 78 ± 9 µm, not shown), whereas only 2 neurons of 23 displayed C fiber-related APs in deeper laminas (mean depth: 445 ± 68 µm). For these two neurons, a stimulation of the RF at voltage higher than 30 V was required, whereas the mean threshold to observe C fiber discharge in control rats was 20 ± 7 V and 20 ± 3 V for superficial and deep dorsal horn neurons, respectively. APs resulting from the stimulation of A-type sensory neurons could be recorded in control and NMD rats. The stimulation thresholds in the recorded spinal neurons were not statistically different for A fibers in control (16 ± 8 V, n = 20) and NMD rats (16 ± 7 V, n = 23; Student's t-test, t_{41} = 0.041; p = 0.9672).

This surprising result led us to attempt single-unit recording of C-type sensory neurons, directly in the DRG of P14 NMD rats. Based on conduction velocity of C-type DRG neurons, we found them to be excitable after RF stimulation (Fig. 1B). As shown in Fig. 1B, C-type DRG neurons typically displayed AP discharge 50–250 ms after stimulation of the RF in control (n = 7; latency to observe APs: 62 ± 2 ms) and NMD rats (n = 13; latency to observe APs: 69 ± 3 ms). However, electrical stimulation thresholds for the induction of APs were significantly higher in NMD rats compared to controls as shown in the histogram of Figure 1B (control: 21 ± 4 V, n = 7; NMD: 52 ± 2 V, n = 13; Student's t-test, t_{18} = 7.79; p < 0.0001). In good agreement with the lack of C-type discharge observed in deep dorsal neurons, corresponding to the criteria of wide dynamic range (WDR) neurons, we failed to see windup plasticity in NMD animals contrary to those recorded from the control group (Fig. 1C and D). As illustrated in the figure, increase in AP discharge frequency producing windup was clearly contributed by the recruitment of slowly conducting C-type sensory neurons in control animals.

This finding indicates that C-type DRG neurons of P14 NMD rats are difficult to recruit and raises the question of a delay in the maturation of sensorispinal nociceptive transmission. Before investigating possible functional mechanisms explaining the absence of C-type sensorispinal transmission in spinal cord neurons, we further characterized the consequences of NMD on the expression of some classical molecular markers of C-type sensory neurons at this postnatal age.

Neurochemical alterations of C-type sensory neuron

On the basis of their neuropeptide content, C-type nociceptors are classically divided into two major neurochemical subtypes: the pep-tidergic neurons containing CGRP (in combination with several other neuropeptides), and the IB4-

binding non-peptidergic neurons (Todd, 2010). To test whether NMD determines phenotypic alterations of these neurons we specifically studied the expression of CGRP and IB4 in lumbar DRGs and spinal dorsal horn.

As expected, the two subtypes were clearly distinguished in control and NMD rats (Fig. 2A and C), but the intensity of the fluorescent signals appeared to be lower in NMD rats (Fig. 2A and C right panels). Accordingly, the fluorescence integrated density of IB4 and CGRP staining was significantly reduced in NMD compared to control rats (IB4: CT: 5.9 ± 0.4, n=5; NMD: 3.3 ± 0.4, n = 5; Mann-Whitney test, p = 0.016 - Figure 2B; CGRP: CT: 5.7 ± 0.4, n = 5; NMD: 4.0 ± 0.3, n = 5; Mann-Whitney test, p = 0.013 - Figure 2D). No significant differences were observed in the density of IB4+ (CT: 257 ± 5 cells/mm^2, n = 5; NMD: 225 ± 14 cells/mm^2, n = 5; Mann-Whitney test, p = 0.117) or CGRP+ neurons (CT: 158 ± 25 cells/mm^2; NMD: 137 ± 15 cells/mm^2, n = 5; Mann-Whitney test, p = 0.251). At the spinal dorsal horn level, IB4 labeled fibers were localized in the ventral part of lamina II (lamina II inner; Fig. 2E), whereas CGRP labeled fibers were localized in lamina I and in the dorsal part of lamina II (lamina II outer; Fig. 2G). Also in this case, the fluorescence integrated density of both IB4 and CGRP was significantly reduced in NMD (IB4: 4.0 ± 0.6; n = 5 - Figure 2F; CGRP: 3.6 ± 6.5; n = 5 - Fig. 2H) as compared to control rats (IB4: 15.0 ± 1.8, n = 4; Mann-Whitney test, p = 0.016 - Fig. 2F; CGRP: 8.1 ± 1.2, n = 4; Mann-Whitney test, p = 0.016 - Figure 2H).

We next investigated whether these phenotypic changes were associated with an altered expression of neurotrophic factor signaling with special emphasis on NGF and GDNF and their respective receptors trkA and RET in NMD rats (Fig. 3). In control animals, expression of NGF transcripts decreased along the developmental period to reach adult-like levels by P24. In NMD rats, the expression of NGF transcripts was much lower at P7 (Student's t-test, t = 6.88; P < 0.001), peaked at P18 and decreased to be not different from that of control at P24. Spinal levels of GDNF mRNA at P7 were extremely low in NMD rats compared to non-NMD controls (Fig. 3A; Student's t-test, t = 6.13; P < 0.001). At P14 and later on, expression levels of GDNF transcripts for GDNF were similar between NMD and control groups. Compared to spinal cord samples of the control group, expression levels found in NMD rats were not different for trkA (Two-way ANOVA, $F_{(3,18)} = 1.992$, p = 0.185) and for RET (Two-way ANOVA, $F_{(3,18)} = 1.969$, p = 0.189) between P4 and P24.

To further investigate changes affecting DRG neurons after NMD with respect to their excitability, we analyzed the expression with time of a set of transcripts coding for two-pore domain K+ channels (K2P) "leak" channels and for voltage-dependent sodium channels. K2P channels are known to hyperpolarize the resting membrane potential and we found that the transcript expression of some of them (Trek2, Tresk and Traak but not Task1) was significantly increased at P14 (i.e. just after the NMD procedure) compared to the control group (Fig. 4A; Two-way ANOVA, $F_{13,84} = 60.70$, P < 0.0001; n = 14). Interestingly, levels for these K2P channels were not different when analyzed at P45 (i.e. after P24 when growth factor transcripts are also normalized). To go one step forward, we also analyzed the corresponding expression of some voltage-dependent Na$^+$ channel transcripts, including those that are specific to C-nociceptors (i.e. Nav1.8, Nav1.9). Whereas Nav1.4 expression remained unchanged between NMD and control animals at P24 and P45 (Fig. 4B), the expression of DRG Nav1.8 and Nav1.9 transcripts was significantly higher in NMD compared to control animals (Two-way ANOVA, $F_{5,36} = 62.68$; P < 0,0001; n = 14). At P45, Nav1.8 transcripts remained significantly higher in NMD animals (Bonferroni, P = 0.0002), whereas Nav1.9 mean level was not different between groups (Bonferroni, P = 0.035).

Increased synaptic inhibition in spinal lamina II neurons of NMD rats

To evaluate the impact of these changes on sensorispinal synapses, we next recorded lamina II neurons in spinal cord slices of control and NMD rats to measure fast synaptic transmission mediated by glutamate and GABA receptor channels (Fig. 5 and Table 1). The analysis of spontaneously occurring EPSCs revealed that, under basal conditions, the mean amplitude and frequency of EPSCs was similar in control and in NMD rats (Student's t-test, $t_{23} = 1.87$, P = 0.07). In addition, we verified if C-type synapses onto lamina II neurons were functional at P14. To do so, we used capsaicin to stimulate the subpopulation of C-type primary afferent fibers classically expressing transient receptor potential vanilloid type 1 (Fig. 5A). Capsaicin (1 lM) significantly increased the frequency of spontaneously occurring EPSCs in lamina II neurons of controls (2.10 ± 0.32 Hz, n = 10; Student's t-test, $t_9 = 4.761$; p = 0.002) and NMD animals (2.03 ± 0.43 Hz, n = 11; Student's t-test, $t_{10} = 2.72$; p = 0.002). This confirmed that capsaicin-sensitive C-type neurons established fully functional synapses with spinal cord neurons in lamina II at P14.

We next focused our attention to inhibitory synaptic transmission ensured by the local inhibitory interneurons. While recording from lamina II neurons at a holding potential of 0 mV (reversal potential for excitatory synaptic currents), we isolated spontaneously occurring inhibitory postsynaptic currents (sIPSCs, Fig. 5B). As indicated in Table 1, the mean frequency of occurrence and deactivation constant (τ) of sIPSCs were similar (frequency: Student's t-test, $t_{14} = 0.20$, P = 0.84; s decay: Student's t-test, $t_{14} = 0.51$, P = 0.62) between controls and NMD rats. However, the mean amplitude of IPSCs was significantly higher in lamina II neurons recorded from the NMD group (Student's t-test, $t_{14} = 3.67$; p =0.003; see also graph in figure 5B) when compared to control. This increase in amplitude corresponded to a higher mean inhibitory charge carried by postsynaptic inhibitory amino acid receptors of 273.7 ± 44.0 pA.ms (n = 9) and of 633.4 ± 64.3 pA.ms (n = 7; Student's t-test, $t_{14} = 4.77$, p = 0.0003) for control and NMD rats, respectively. According to these data, the elevated inhibitory synaptic tone in lamina II might have been responsible for the absence of C-type AP discharge seen in II order spinal cord neurons of P14 NMD rats.

C-type nociceptive messages do not excite WDR neurons of NMD rats at P14 due to excessive spinal inhibitory barrage

Results above should, however, be considered with caution since whole-cell patch-clamp conditions are set at the chloride equilibrium potential which is subject to well-described developmental changes. It remains that the increased GABAergic inhibition might significantly contribute to a shunting inhibition, as classically-described for PAFs, irrespective of the developmental stage. To further support this hypothesis, we administered selective antagonists of GABA$_A$ (gabazine, 1 µM) and glycine (strychnine, 10 µM) receptors while recording *in vivo* the AP discharges of single neuronal units in the spinal cord after stimulation of the peripheral RF (Figure 6A).

In deep dorsal horn WDR neurons (depth: 609 ± 29 µm), the application of gabazine and/or strychnine allowed to detect C fiber-evoked APs and re-established windup plasticity in all neurons recorded (Figure 6A, n = 9). In neurons

of superficial laminae of dorsal horn (depth: 91 ± 6 µm), we also revealed the presence of C-mediated AP discharge after bicuculline or strychnine spinal application (n = 7, not shown). As indicated in figure 6B, the C fiber mean threshold was of 42 ± 2 V in the presence of strychnine, of 38 ± 2 V after gabazine and of 37 ± 1 V when gabazine and strychnine were co-applied (Two-way ANOVA, $F_{(3,24)} = 59.14$, $p < 0.0001$). In line with our patch-clamp data on lamina II neurons, we did observe a capsaicin-induced increase in AP discharge in theses neurons that was similar to the one observed in controls (about thirteen-fold increase; n = 5 neurons out of 7, not shown). These results were not reproduced by local application of the vehicle for bicuculline, strychnine, or capsaicin (NaCl 0.9%, not shown).

Long-term consequences of NMD history on rat mechanical and thermal nociception

Neonatal maternal deprivation was characterized by a lack of C-type sensory-spinal transmission when measured in second-order spinal neurons of rats. This likely explained the absence of windup plasticity while recording from WDR neurons in NMD rats at P14 after repetitive electrical stimulation of the RF. As illustrated in Fig. 7A, windup appeared to have fully recovered at P24. This raised several concerns, particularly related potential to long-term consequences of NMD history on nociception. We then measured nociceptive thresholds in control and NMD rats from postnatal day 24 to 100. Compared to the control group of rats (Fig. 7B), we found that NMD rats exhibited significantly lower mechanical (Two-way ANOVA, $F_{2,18} = 139.6$; $P < 0.0001$; n = 10 animals/group) and heat nociceptive thresholds (Two-way ANOVA, $F_{2,18} = 37.65$; $P < 0.0001$; n = 10 animals/group). This strongly suggested that exposing rat neonates to NMD misshaped or triggered long-term changes in the nociceptive system, at least in sensory neurons and second-order spinal neurons.

Discussion

In this work, we provide anatomical and functional evidence indicating that NMD affects the early postnatal development of the spinal nociceptive system and possibly the setting of nociceptive thresholds at adulthood. NMD history is associated with (i) hypoexcitability of C-type DRG neurons 2 weeks after birth that is related to an elevated inhibitory barrage in lamina II of the spinal cord, preventing the activation of second-order spinal neurons by C fibers, (ii) an alteration of the excitatory/inhibitory balance in lamina II neurons, (iii) an alteration of the neurochemical properties of C-type fibers located in lamina II of the spinal cord dorsal horn that could be associated with (iv) changes in the expression of growth factors responsible for the functional establishment of C-type fibers, (v) changes in the expression of channels setting sensory neuron excitability and (vi) the outcome at the behavioral level, i.e. the hypersensitivity of NMD animals when exposed to a noxious stimulus in adulthood. Altogether, these data support the hypothesis that NMD not only strongly alters the maturation of C-type sensory-spinal transmission but also increases the duration of the temporary period in which A-type sensory neurons processes nociceptive input to the spinal cord. After a delay of about 10 days, C-type sensory-spinal transmission to second-order neurons seems to have fully recovered, but rats with NMD history remained hypersensitive to noxious mechanical and heat stimulation.

It has been shown that the maturation of the spinal nociceptive system in rats occurs mainly during the early postnatal period. Notably, C-type PAFs are already present in the grey matter of the spinal cord at birth and even establish synaptic contacts during the embryonic period. These contacts seem, however, capable of exciting the second-order spinal cord neurons only from P10 onward (Fitzgerald & Gibson, 1984). The maturation of C-type PAFs is a complex process involving NGF and GDNF for peptidergic and non-peptidergic nociceptors, respectively. An increase in neurotrophic factor expression (Chung et al., 2007) as a consequence of deficits in maternal care during the pre-weaning period (such is the case of NMD) has been indicated to contribute to the visceral hyperalgesia that is observed at subsequent ages. However, at least to our knowledge very few studies have investigated the short-term effects of NMD during the critical time window of the nociceptive system maturation during the first weeks after birth. Here, we show that NMD induced a delay in the maturation of C-type PAFs, as we failed to observe any C fiber discharge in spinal cord nociceptive-specific neurons and a corresponding impossibility to produce windup in WDR neurons. The absence of windup is directly correlated with the lack of C-type PAF-evoked APs, in keeping with the observation that this progressive depolarization of the postsynaptic membrane cannot be produced by A fibers in young or adult spinal cord under normal conditions (Fitzgerald, 1987)

One of the major findings of this work came from recording of C-type nociceptors in the DRG of NMD rats. C-nociceptors were indeed excitable but required very high intensities of stimulation (about twice more than control animals) of the RF to exhibit APs. This fits well with the increased expression of K2P channel transcripts which could maintain a low resting membrane potential, if translated in proteins, and directly participate to set nociceptive thresholds, as previously demonstrated [for review see Li & Toyoda (2015)]. In addition to this possible mechanism, we also hypothesize that the transfer of nociceptive messages to high-order neurons was inhibited as we failed to observe APs in these neurons after electrical stimulation of RF or following topical application of capsaicin. The inhibitory barrage-related hypothesis was confirmed by recording IPSCs in lamina II neurons. Compared to non-deprived animals, IPSCs from NMD rats were of greater amplitude and carried more inhibitory charge. These data are in good agreement with the delay hypothesis as it has been shown previously that the response to capsaicin progressively increases during the first 10 postnatal days in rat (Baccei et al., 2003). The strength of synaptic inhibition mediated by $GABA_A$ and/or glycine receptors has been shown to decrease with age (Keller et al., 2001; Baccei & Fitzgerald, 2004), but can be reactivated in pathological conditions including inflammatory pain conditions (Poisbeau et al., 2005), or exhibit long-term plasticity after neonatal injury (Li et al., 2013). The fact that we found a significant increase in synaptic inhibition in NMD rats compared to controls further supports the idea of a delay in the maturation steps, leading to an adult-like state of spinal inhibition in the dorsal horn while processing nociceptive messages. The idea of a functional delay in the maturation of C fiber is further supported by the reduction in staining intensity of IB4 and CGRP in the superficial laminas of the dorsal horn in NMD rats. Although the neurochemical pattern of C fibers is also subjected to maturation-related modifications (Lorenzo et al., 2008), our data indicate that NMD somehow influences this pattern toward a higher degree of immaturity.

In addition to the peripheral effects of NMD, our functional and neurochemical findings suggest that the elevated GABA/glycine receptor-mediated inhibition contributes strongly to the lack of detection of C-type PAFs at P14. As a consequence, we could speculate that nociceptive information taken in charge physiologically by A-type fibers during

this early developmental period (Fitzgerald, 2005) will be prolonged, and possibly render nociceptive circuits hypersensitive at adulthood. This is indeed the case as mechanical and thermal heat nociceptive thresholds are significantly reduced in NMD rats from P24 to P100. It is tempting to speculate that the long-lasting increase in Nav1.8 expression, a C-type specific voltage-dependant excitatory channel in DRG, participates to nociceptive hypersensitivity. This idea fits well with the role of Nav1.8 current in C-type DRG neurons which contribute to most of the depolarizing phase of APs and control the repetitive firing in these neurons (Renganathan et al., 2001).

Taken together, our results demonstrate that an aversive early life event, such as the psychological stress of NMD occurring during the early postnatal period in rats (corresponding to the last trimester of gestation in humans), may lead to significant alterations in the functional establishment of nociceptive pathways. Abnormal inhibitory control of spinal nociceptive messages during this critical postnatal window may be of significant importance in the framework of nociceptive processing and pain sensitivity in adult-hood (Koch & Fitzgerald, 2013). With regards to additional deleterious consequences of NMD on psychosocial, emotional and addictive behaviors, a better understanding of the powerful long- lasting mechanisms underlying these changes will certainly contribute to improve the clinical care of neonates placed in intensive care units and to the prevention of perinatal stress-related health problems in later life.

Conflict of interests

The authors declare no competing financial interests.

Acknowledgments

Abbreviations

APs, action potentials; CGRP, calcitonin gene-related peptide; DRG, dorsal root ganglion; EPSCs, excitatory postsynaptic channels; GDNF, glial-derived neurotrophic factor; IB4, isolectin B4; IPSCs, inhibitory postsynaptic currents; K2P, two-pore domain K+ channels; NGF, nerve growth factor; NMD, neonatal maternal deprivation; PAFs, primary afferent fibers; RF, receptive field; WDR, wide dynamic range.

References

Baccei, M.L. & Fitzgerald, M. (2004) Development of GABAergic and glycinergic transmission in the neonatal rat dorsal horn. J. Neurosci., 24, 4749–4757.

Baccei, M.L., Bardoni, R. & Fitzgerald, M. (2003) Development of nociceptive synaptic inputs to the neonatal rat dorsal horn: glutamate release by capsaicin and menthol. J. Physiol., 549, 231–242.

Bayer, S.A., Altman, J., Russo, R.J. & Zhang, X. (1993) Timetables of neurogenesis in the human brain based on experimentally determined patterns in the rat. Neurotoxicology, 14, 83–144.

Bennett, D.L., Averill, S., Clary, D.O., Priestley, J.V. & McMahon, S.B. (1996) Postnatal changes in the expression of the trkA high-affinity NGF receptor in primary sensory neurons. Eur. J. Neurosci., 8, 2204– 2208.

Bertin, D., Jourde-Chiche, N., Bongrand, P. & Bardin, N. (2013) Original approach for automated quantification of antinuclear autoantibodies by indirect immunofluorescence. Clin. Dev. Immunol., 2013, 182172.

Chung, E.K., Zhang, X.J., Xu, H.X., Sung, J.J. & Bian, Z.X. (2007) Visceral hyperalgesia induced by neonatal maternal separation is associated with nerve growth factor-mediated central neuronal plasticity in rat spinal cord. Neuroscience, 149, 685–695.

Fitzgerald, M. (1987) Cutaneous primary afferent properties in the hind limb of the neonatal rat. J. Physiol., 383, 79–92.

Fitzgerald, M. (1988) The development of activity evoked by fine diameter cutaneous fibres in the spinal cord of the newborn rat. Neurosci. Lett., 86, 161–166.

Fitzgerald, M. (2005) The development of nociceptive circuits. Nat. Rev. Neurosci., 6, 507–520.

Fitzgerald, M. & Gibson, S. (1984) The postnatal physiological and neuro-chemical development of peripheral sensory C fibres. Neuroscience, 13, 933–944.

Hargreaves, K., Dubner, R., Brown, F., Flores, C. & Joris, J. (1988) A new and sensitive method for measuring thermal nociception in cutaneous hyperalgesia. Pain, 32, 77–88.

Jennings, E. & Fitzgerald, M. (1998) Postnatal changes in responses of rat dorsal horn cells to afferent stimulation: a fibre-induced sensitization. J. Physiol., 509(Pt 3), 859–868.

Juif, P.E. & Poisbeau, P. (2013) Neurohormonal effects of oxytocin and vasopressin receptor agonists on spinal pain processing in male rats. Pain, 154, 1449–1456.

Keller, A.F., Coull, J.A., Chery, N., Poisbeau, P. & De Koninck, Y. (2001) Region-specific developmental specialization of GABA-glycine cosynapses in laminas I-II of the rat spinal dorsal horn. J. Neurosci., 21, 7871–7880.

Kikusui, T. & Mori, Y. (2009) Behavioural and neurochemical consequences of early weaning in rodents. J. Neuroendocrinol., 21, 427–431.

Koch, S.C. & Fitzgerald, M. (2013) Activity-dependent development of tactile and nociceptive spinal cord circuits. Ann. N. Y. Acad. Sci., 1279, 97– 102.

Ladd, C.O., Huot, R.L., Thrivikraman, K.V., Nemeroff, C.B., Meaney, M.J. & Plotsky, P.M. (2000) Long-term behavioral and neuroendocrine adaptations to adverse early experience. Prog. Brain Res., 122, 81–103.

Lelievre, V., Hu, Z., Byun, J.Y., Ioffe, Y. & Waschek, J.A. (2002) Fibroblast growth factor-2 converts PACAP growth action on embryonic hindbrain precursors from stimulation to inhibition. J. Neurosci. Res., 67, 566–573.

Li, X.Y. & Toyoda, H. (2015) Role of leak potassium channels in pain signaling. Brain Res. Bull., 119, 73–79.

Li, H., Tornberg, J., Kaila, K., Airaksinen, M.S. & Rivera, C. (2002) Patterns of cation-chloride cotransporter expression during embryonic rodent CNS development. Eur. J. Neurosci., 16, 2358–2370.

Li, J., Blankenship, M.L. & Baccei, M.L. (2013) Deficits in glycinergic inhibition within adult spinal nociceptive circuits after neonatal tissue damage. Pain, 154, 1129–1139.

Lorenzo, L.E., Ramien, M., St Louis, M., De Koninck, Y. & Ribeiro-da-Silva, A. (2008) Postnatal changes in the Rexed lamination and markers of nociceptive afferents in the superficial dorsal horn of the rat. J. Comp. Neurol., 508, 592–604.

Luis-Delgado, O.E., Barrot, M., Rodeau, J.L., Schott, G., Benbouzid, M., Poisbeau, P., Freund-Mercier, M.J. & Lasbennes, F. (2006) Calibrated forceps: a sensitive and reliable tool for pain and analgesia studies. J. Pain, 7, 32–39.

Mendell, L.M. (1966) Physiological properties of unmyelinated fiber projection to the spinal cord. Exp. Neurol., 16, 316–332.

Plotsky, P.M. & Meaney, M.J. (1993) Early, postnatal experience alters hypothalamic corticotropin-releasing factor (CRF) mRNA, median eminence CRF content and stress-induced release in adult rats. Brain Res. Mol. Brain Res., 18, 195–200.

Poisbeau, P., Patte-Mensah, C., Keller, A.F., Barrot, M., Breton, J.D., Luis-Delgado, O.E., Freund-Mercier, M.J., Mensah-Nyagan, A.G. et al. (2005) Inflammatory pain upregulates spinal inhibition via endogenous neurosteroid production. J. Neurosci., 25, 11768–11776.

Renganathan, M., Cummins, T.R. & Waxman, S.G. (2001) Contribution of Na(v)1.8 sodium channels to action potential electrogenesis in DRG neurons. J. Neurophysiol., 86, 629–640.

Rivera, C., Voipio, J., Payne, J.A., Ruusuvuori, E., Lahtinen, H., Lamsa, K., Pirvola, U., Saarma, M. et al. (1999) The K^+/Cl co-transporter KCC2 renders GABA hyperpolarizing during neuronal maturation. Nature, 397, 251–255.

Ruit, K.G., Elliott, J.L., Osborne, P.A., Yan, Q. & Snider, W.D. (1992) Selective dependence of mammalian dorsal root ganglion neurons on nerve growth factor during embryonic development. Neuron, 8, 573– 587.

Salio, C., Lossi, L., Ferrini, F. & Merighi, A. (2005) Ultrastructural evidence for a pre- and postsynaptic localization of full-length trkB receptors in substantia gelatinosa (lamina II) of rat and mouse spinal cord. Eur. J. Neurosci., 22, 1951–1966.

Schwaller, F. & Fitzgerald, M. (2014) The consequences of pain in early life: injury-induced plasticity in developing pain pathways. Eur. J. Neurosci., 39, 344–352.

Stil, A., Liabeuf, S., Jean-Xavier, C., Brocard, C., Viemari, J.C. & Vinay, L. (2009) Developmental up-regulation of the potassium-chloride cotransporter type 2 in the rat lumbar spinal cord. Neuroscience, 164, 809–821.
Todd, A.J. (2010) Neuronal circuitry for pain processing in the dorsal horn. Nat. Rev. Neurosci., 11, 823–836.

Tsang, S.W., Zhao, M., Wu, J., Sung, J.J. & Bian, Z.X. (2012) Nerve growth factor-mediated neuronal plasticity in spinal cord contributes to neonatal maternal separation-induced visceral hypersensitivity in rats. Eur. J. Pain, 16, 463–472.

Urch, C.E. & Dickenson, A.H. (2003) In vivo single unit extracellular recordings from spinal cord neurones of rats. Brain Res. Brain Res. Protoc., 12, 26–34.

White, M.C. & Wolf, A.R. (2004) Pain and stress in the human fetus. Best Pract. Res. Clin. Anaesthesiol., 18, 205–220.
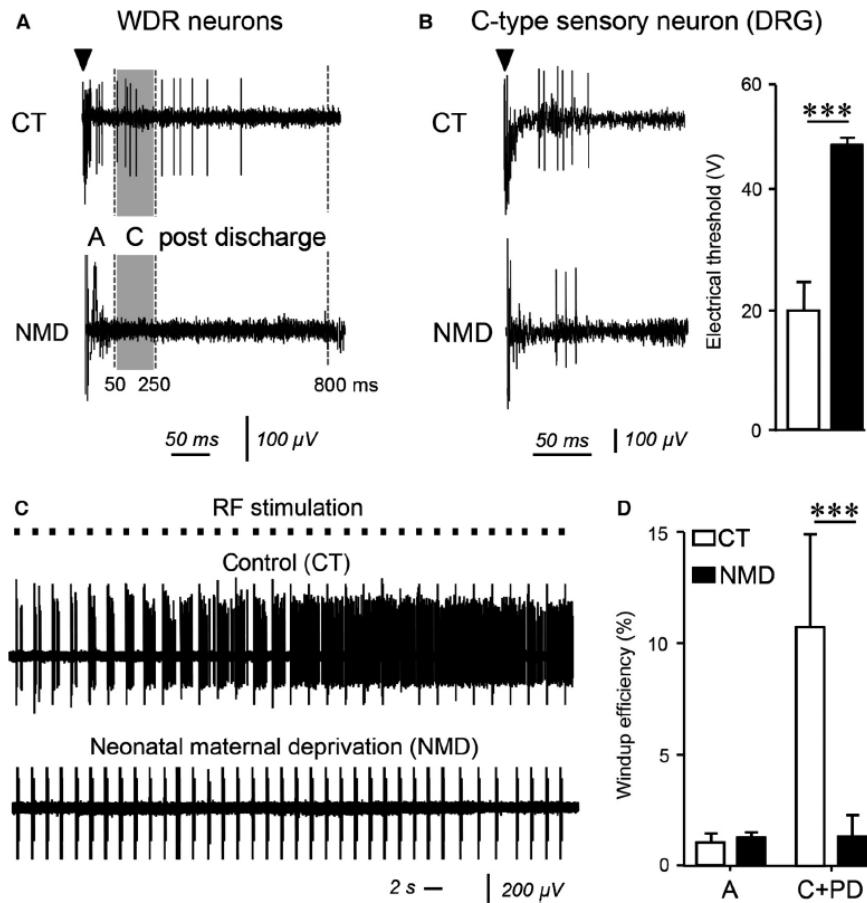
Figure 1

FIG. 1. (A) Representative traces illustrating single-unit extracellular voltage responses of WDR spinal neurons located in deep dorsal horn laminas following a single electrical stimulation of peripheral RF in control (top) and NMD (bottom) animals. The grey box indicates the expected latency to observe C fiber action potentials at P14. (B) Typical extracellular recording of C-type sensory neurons in the DRG of control and NMD animals, after single electrical stimulation of peripheral RF. Note that both neurons displayed an action potential discharge. The graphs on the right shows the electrical stimulation thresholds required for the activation of these C-type sensory neuron in control (white bar) and NMD animals (black bar). (C) Representative traces of action potential firing activity recorded from WDR neurons during a train of 30 repetitive stimulations of the peripheral receptive field (RF stimulation: 1 Hz, three times C fiber threshold). A strong increase in the number of action potentials was observed with time in control animals (top trace) corresponding to a windup phenomenon. No such increase was observed in neonatal maternally deprived (NMD) animals (bottom trace). (D) Graph showing windup efficiency with respect to fiber type: A fiber discharge (0–50 ms following the artifact of stimulation) remained unchanged in both groups, whereas the number of C fiber (50–800 ms after the artifact of stimulation) action potentials was significantly increased in control animals compared to NMD rats. Statistical code for Student's t-test (control vs. NMD): ***$P < 0.001$.
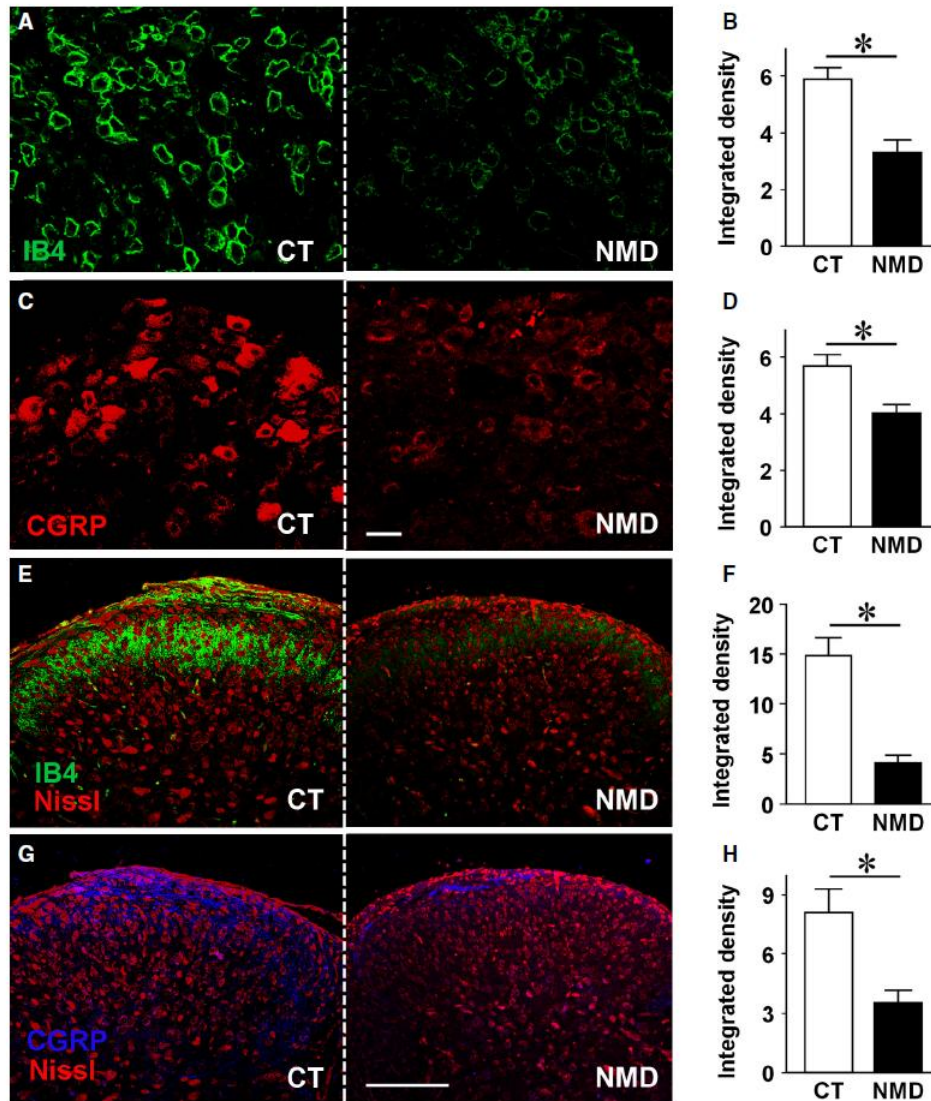
Figure2:

FIG. 2. Immunofluorescence analysis of IB4 and CGRP staining in DRGs and spinal dorsal horn. (A) IB4 fluorescence is strongly reduced in small-to-medium size non-peptidergic DRG neurons of NMD rats (right image) compared to control (CT, left image). (B) Bar chart illustrating the reduction in IB4 fluorescence integrated density in NMD rats (Mann–Whitney test, $P = 0.016$). (C) CGRP fluorescence is strongly reduced in small-to-medium size peptidergic DRG neurons of NMD rats (right image) compared to CT (left image). (D) Graph showing the reduction in CGRP fluorescence integrated density in NMD rats compared to controls (Mann–Whitney test, $P = 0.013$). (E) Reduction in IB4 fluorescence in non-peptidergic nociceptive fibers of the superficial dorsal horn of NMD rats (right image) compared to CT (left image). (F) Bar chart illustrating the reduction in IB4 fluorescence integrated density in NMD rats (Mann–Whitney test, $P = 0.016$). (G) Reduction in CGRP fluorescence in peptidergic nociceptive fibers of the superficial dorsal horn of NMD rats (right image) compared to control (CT, left image). (H) Bar chart showing the reduction in CGRP fluorescence intensity in NMD rats (Mann–Whitney test, $P = 0.016$). (E–G) Nissl staining (red) was used together with IB4 or CGRP to better identify spinal lamination. IB4, isolectin B4; CGRP, calcitonin gene-related peptide; CT, control; NMD, neonatal maternal deprivation. Scale bars: (A, C): 40 μm; (E, G): 200 μm.
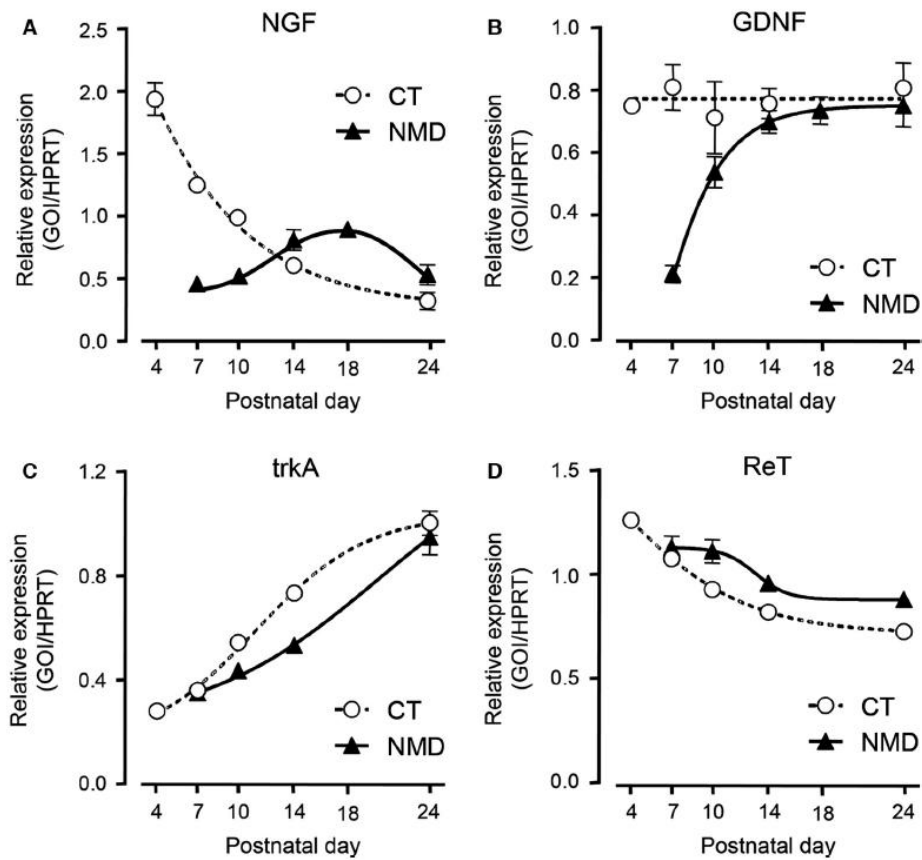
Figure 3:

FIG. 3. Changes in the expression levels of NGF, GDNF, trkA and RET transcripts from P4 to P24, in the spinal cord of control (CT) and NMD rats. Data for the gene of interest (GOI) are expressed relative to the housekeeping gene HPRT. Statistical code: *$P < 0.05$; ***$P < 0.001$ control vs. NMD.
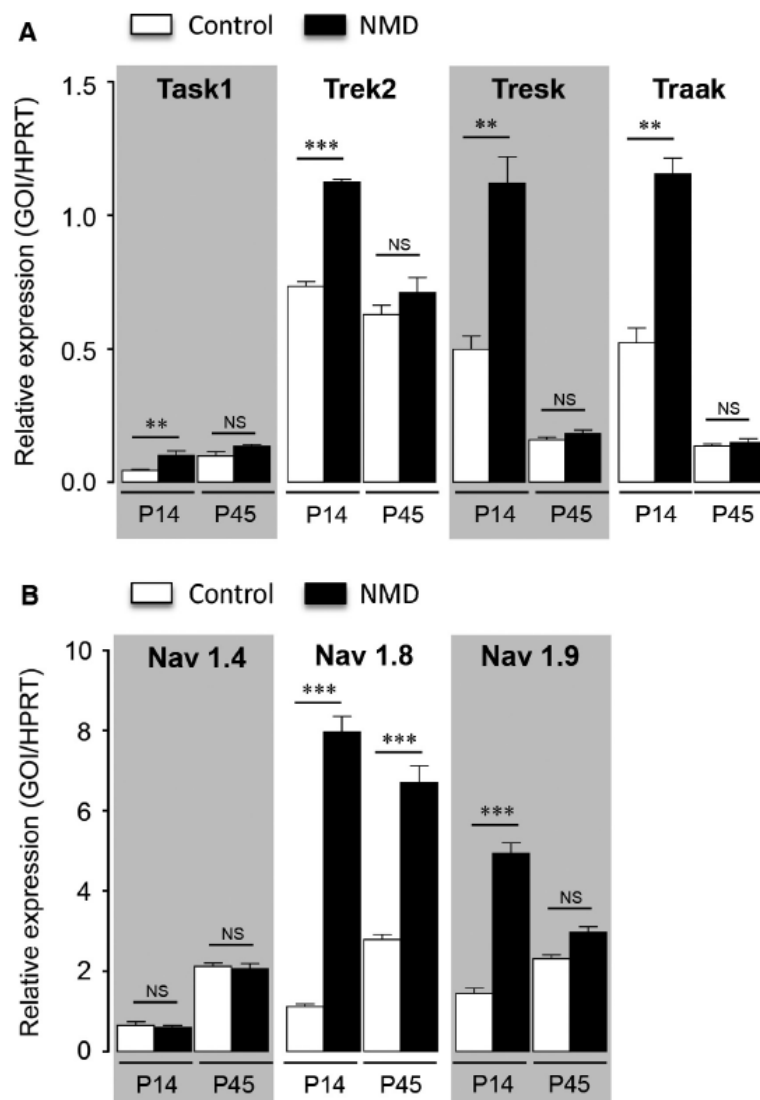
Figure 4:

FIG. 4. (A) Changes in the expression levels of several K2P "leak" channels (Task1, Trek2, Tresk, Traak) and (B) of some voltage-dependent Nav (iso-forms 1.4, 1.8, 1.9) in the DRG of control (CT) and NMD rats at P14 and P45. Data for each gene of interest (GOI) are expressed relative to the house-keeping gene HPRT. Statistical code for Bonferroni multiple comparisons: $**P < 0.01$; $***P < 0.001$ control vs. NMD.
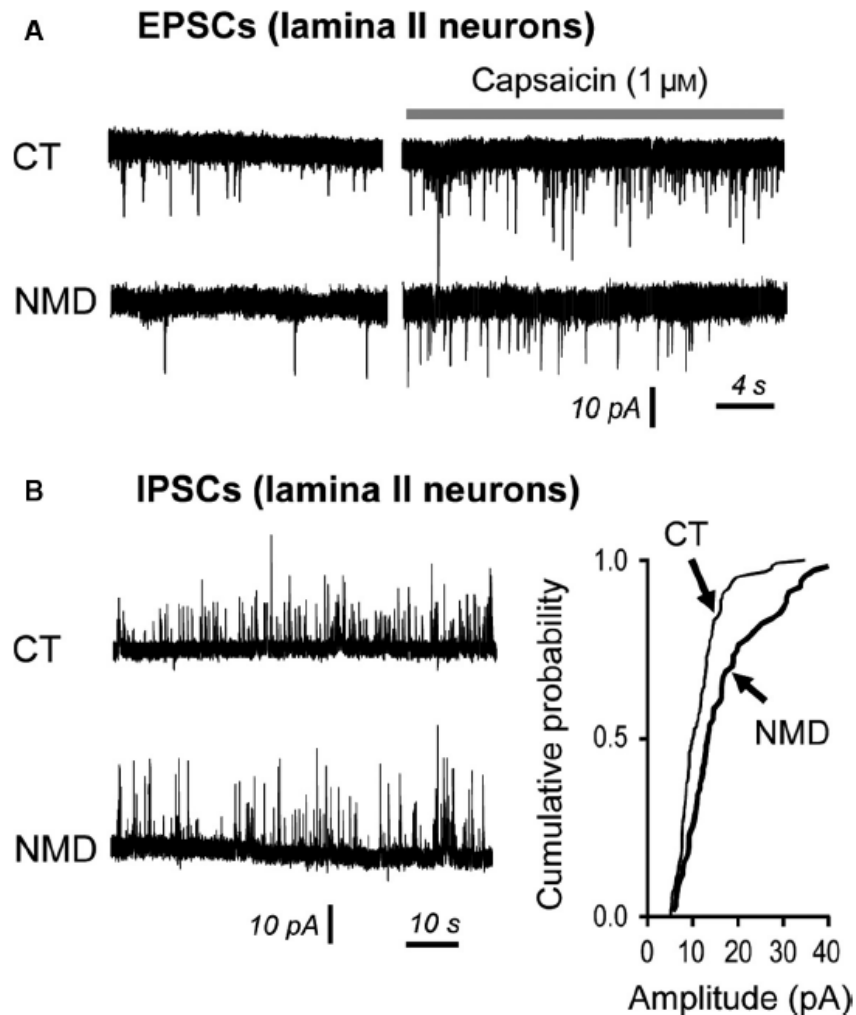
Figure 5:

FIG. 5. Characteristics of inhibitory and excitatory synaptic controls on lamina II neurons at P14. (A) Left traces illustrate a typical patch-clamp recording of lamina II neurons, at a voltage holding of – 60 mV, from spinal cord slices of control (CT) and NMD rats. Excitatory postsynaptic channels (EPSCs) are seen as inward currents in basal condition and in the presence of capsaicin (1 μM). Grey bar indicates duration of the slice superfusion with capsaicin. (B) Recording of lamina II neurons at a holding potential of 0 mV showing transient outward currents corresponding to inhibitory postsynaptic currents (IPSCs). Amplitude distribution of IPSCs is shown for the illustrated lamina II neurons (control: thin line, $n = 125$; NMD: thick line, $n = 67$). Note that Kolmogorov–Smirnov statistics, comparing the two population, were highly significant ($P < 0.001$).
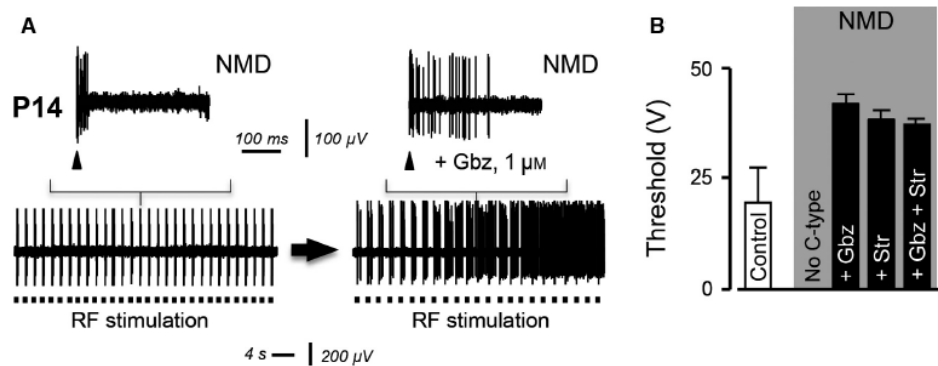
Figure 6

FIG. 6. (A) Representative recording of action potential firing activity recorded from WDR spinal cord neurons of P14 NMD rats in control conditions and after a local application of gabazine (Gbz, 1 µM). (B) Bar chart illustrating C fiber activation thresholds of P14 WDR neurons recorded from control rats (white bar), and NMD rats (grey bars) in the absence of antagonist (no C fiber-mediated APs) and following spinal application of gabazine (Gbz, 1 µM), strychnine (Str, 1 µM) or both antagonists (+ Gbz + Str).
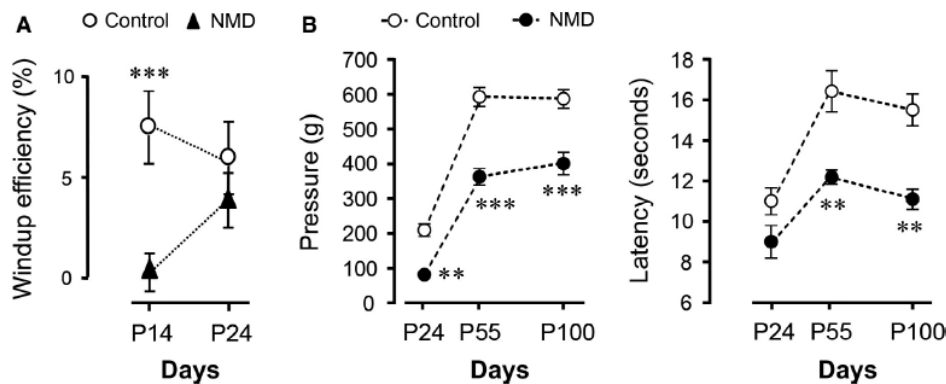
Figure 7:

FIG. 7. (A) Windup efficiency in WDR neurons recorded from control and NMD rats. Note that windup was fully recovered at P24 and did not differ from control rats at this age. (B) Time course of mechanical (left graph) and heat nociceptive thresholds (right graph) for control and NMD rats. Statistical code for Bonferroni multiple comparisons: **$P < 0.01$; ***$P < 0.001$ control vs. NMD at a given time point.

Table1:

TABLE 1. Characteristics of excitatory and inhibitory postsynaptic channels (EPSCs and IPSCs, respectively) recorded from lamina II neurons in the spinal cord of control and NMD rats at P14. Data are presented as mean (SEM). Statistical significance with Student's t-test is indicated by bold values if $P < 0.05$ (**$P < 0.01$)

	Frequency (Hz)	Amplitude (pA)	Decay (ms)
EPSCs			
Control, $n = 15$	0.96 ± 0.29	10.8 ± 1.0	8.4 ± 1.0
NMD, $n = 10$	0.49 ± 0.16	9.3 ± 1.0	9.1 ± 0.7
IPSCs			
Control, $n = 9$	1.01 ± 0.26	9.3 ± 1.6	35.1 ± 3.5
NMD, $n = 7$	0.92 ± 0.34	**17.2 ± 1.3****	38.1 ± 4.9